

Simulation Analysis of Earthquake Response of Onagawa Nuclear Power Plant to the 2011 off the Pacific Coast of Tohoku Earthquake



Kiyoshi Hirotani

Manager, Dept. of Civil & Architectural Engineering, Tohoku Electric Power Co., Inc., Sendai, Japan

Yoshihiro Ogata

Assistant manager, Dept. of Civil & Architectural Engineering, Tohoku Electric Power Co., Inc., Dr. Eng., Sendai, Japan

Hiroshi Otake

Assistant manager, Dept. of Civil & Architectural Engineering, Tohoku Electric Power Co., Inc., Sendai, Japan

Jun Iida

Assistant manager, Dept. of Nuclear Power, Tohoku Electric Power Co., Inc., Sendai, Japan

SUMMARY:

On March 11 in 2011, the nuclear power plant of Tohoku Electric Power Co. in Onagawa (hereafter “Onagawa NPP”) shut down automatically by the 2011 off the Pacific Coast of Tohoku Earthquake (hereafter “March 11 Quake”). This was the largest quake ever experienced by the Onagawa NPP.

We report on the simulation analysis of the nuclear reactor building of Onagawa NPP Unit No. 3 based on the acceleration records taken of the building during the March 11 Quake and the Miyagi Offshore Earthquake of April 7, 2011 aftershock (hereafter “April 7 Quake”), and seismic safety of the building.

Keywords: the 2011 off the Pacific Coast of Tohoku Earthquake, Onagawa NPP, simulation analysis

1. HYPOCENTER LOCATION RELATIVE TO ONAGAWA SITE

Fig. 1 shows the specifications of the March 11 Quake and the April 7 Quake, and the hypocenter locations relative to Onagawa Site of each quake.

Occurrence date and time:
Approx. 14 hr 46 min, Mar. 11, 2011
Earthquake name: March 11 Quake
Epicenter location name: Sanriku Offshore
Magnitude: 9.0
Epicenter location: 38° 6.2' N and 142° 51.6' E
Hypocentral depth: 24 km
Epicenter distance: 123 km
Hypocentral distance: 125 km

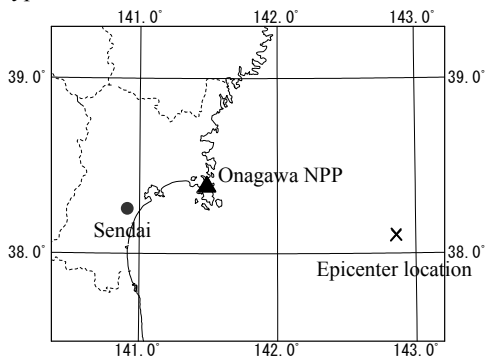


Figure 1.1. Hypocenter lctn relative to Onagawa Site (Mar. 11 Quake)

Occurrence date and time:
Approx. 23 hr 32 min, Apr. 7, 2011
Epicenter location name: Miyagi Offshore
Magnitude: 7.2
Epicenter location: 38° 12.3' N and 141° 55.2' E
Hypocentral depth: 66 km
Epicenter distance: 43 km
Hypocentral distance: 78 km

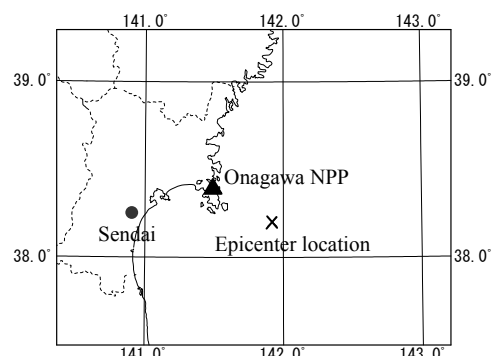


Figure 1.2. Hypocenter lctn relative to Onagawa Site (Apr. 7 Quake)

2. QUAKE OBSERVATION POINTS IN NUCLEAR REACTOR BUILDING

The nuclear reactor building of Onagawa NPP Unit No. 3 is a RC building (partially SRC and steel structure building), 64.6 m high from the basemat slab bottom (35.7 m above the ground level) and with a floor plan dimensions of 80.5 m by 77.0 m (outer surface of BF3 external wall). Fig. 2 shows the quake observation points used in our investigation.

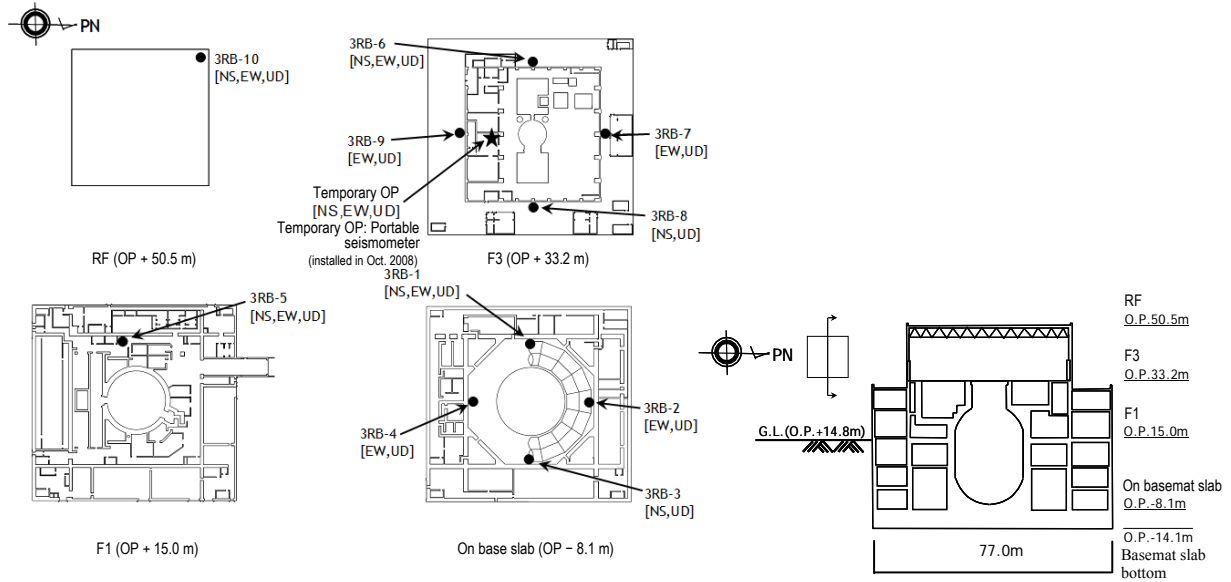


Figure 2. Quake observation points

3. QUAKE OBSERVATION RECORDS

Fig. 3 shows the acceleration waveforms in the observation records on the basemat slab; Fig. 4 shows the maximum acceleration distribution. The March 11 Quake showed a higher maximum acceleration on the basemat slab than the April 7 Quake; the maximum accelerations on the building top were similar between the two quakes. The maximum vertical acceleration on a part of the third floor was greater in the April 7 Quake than in the March 11 Quake because the seismometer happened to be installed at a location particularly susceptible to amplification of vertical vibration.

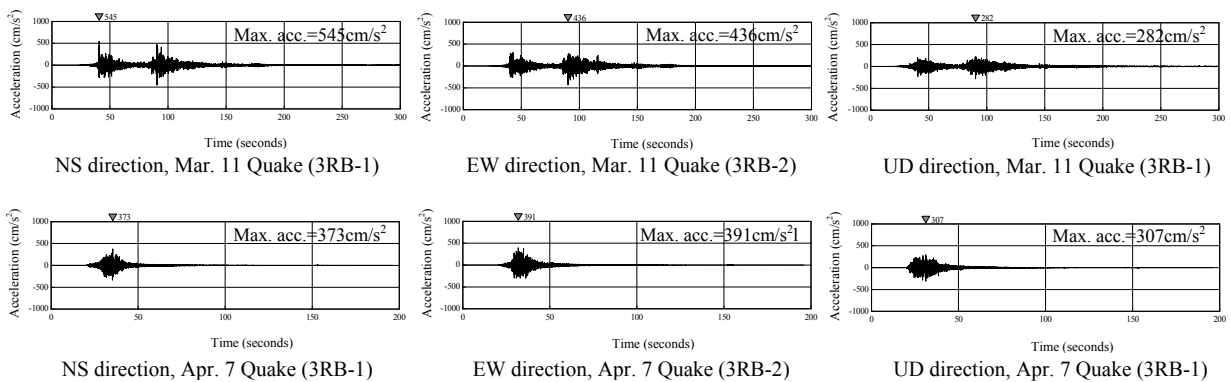


Figure 3. Seismic acceleration waveforms recorded on basemat slab

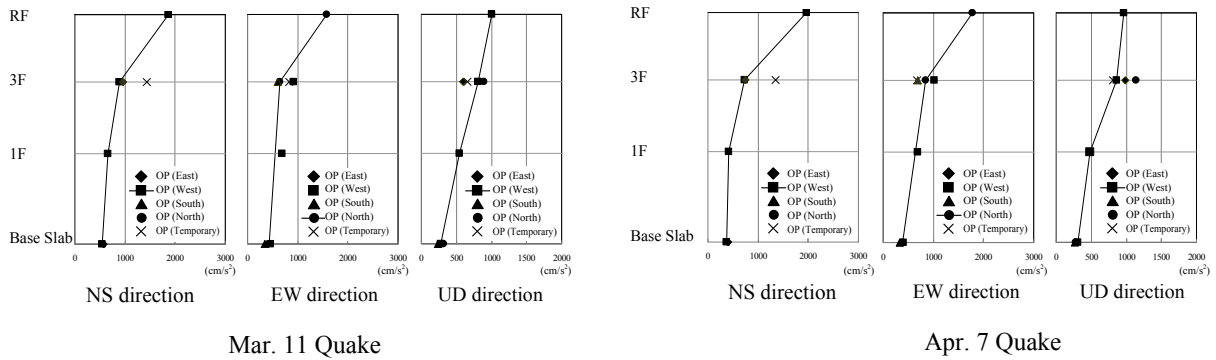


Figure 4. Max. response acceleration distribution

4. SEISMIC RESPONSE ANALYSIS BASED ON PREEXISTING MODEL

We conducted a seismic response analysis using a preexisting model derived from the design model. The preexisting analysis model for the building was a model that used a multi-cantilever and multi-lumped mass system with the rigid basemat slab and main earthquake-resisting walls (box walls and shell walls) substituted by equivalent bending-shear beams. The soil-structure interaction was treated as a dynamic complex stiffness, and analysis was based on vibration admittance theory for rock beneath the building, and the effects of the underground surrounding soil of the side wall are ignored. We performed a frequency response analysis based on the observation records taken on the basemat slab to inversely calculate the input motion from outside the bottom spring for nonlinear time-history seismic response analysis.

Fig. 5 compares the rooftop and third floor acceleration response spectra in the seismic response analysis results for the March 11 Quake with the quake observation records. The analysis largely reproduced the tendencies in the observation records except for those on the short period side. The predominant periods in the observation records are closer to the long period side than those in the analysis results, resulting in poor fitting around the peaks around the 0.1-second period for the rooftop. Additionally, the analysis failed to reproduce the third floor peaks around the 0.1-second period at the temporary observation point for the NS direction and at 3RB-6 for the EW direction. The reproducibility of the RF records posed a problem to the preexisting quake simulation in which the building responses remained in the elastic range.

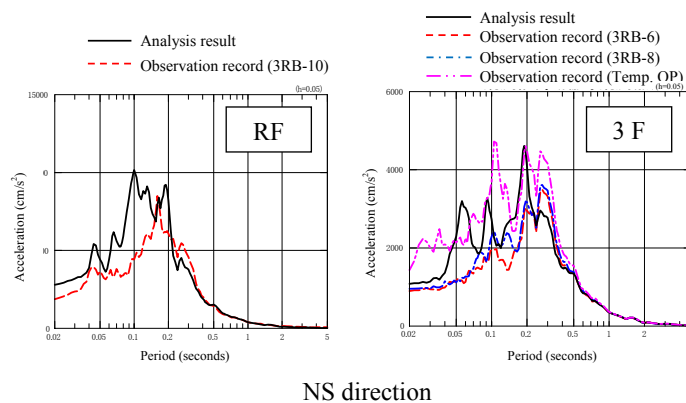


Figure 5.1. Results of seismic response analysis based on preexisting model (Mar. 11 Quake)

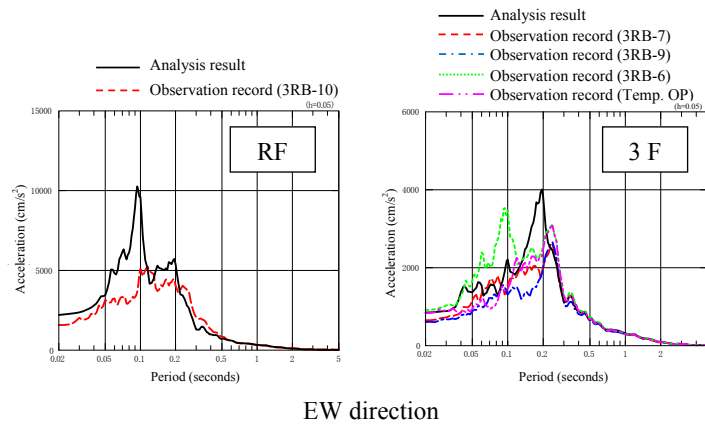


Figure 5.2. Results of seismic response analysis based on preexisting model (Mar. 11 Quake)

5. CREATION OF SIMULATION ANALYSIS MODEL

We improved the analysis model on examination of the vibration characteristics of the reactor building, because the seismic response analysis using a preexisting model did not reproduce the tendencies in the observation with sufficient accuracy.

5.1. Post-Quake Changes in Natural Frequency and Damping Factor of Reactor Building

The natural frequencies and damping factors of reactor building immediately after construction (Onagawa Unit No. 3 put into commercial operation on Jan. 30, 2002) and those based on major earthquake observation records in Onagawa NPP were determined, using the ARX model under the sway-fixed conditions. Table 1 shows the summary of these values. The natural frequency lowered steadily after each quake as compared with immediately after construction, then sharply dropped after the March 11 Quake, and remained more or less similar after April 7 Quake. The damping factor was high after the March 11 Quake and the April 7 Quake than before the March 11 Quake.

Fig. 6 compares the NS-direction rooftop acceleration response spectra during the first and second halves of the principal shock of the March 11 Quake with those during the April 7 Quake. The predominant period of approx. 0.2 seconds and those of 0.1 to 0.2 seconds during the first half of the March 11 Quake became longer during the second half. The April 7 Quake showed a predominant period similar to that of the second half of the March 11 Quake. The quake observation records taken on the basemat slab during the March 11 Quake revealed that the seismic vibration input to the building contained more long-period components in the second half than in the first half. This is reflected in Fig. 6.

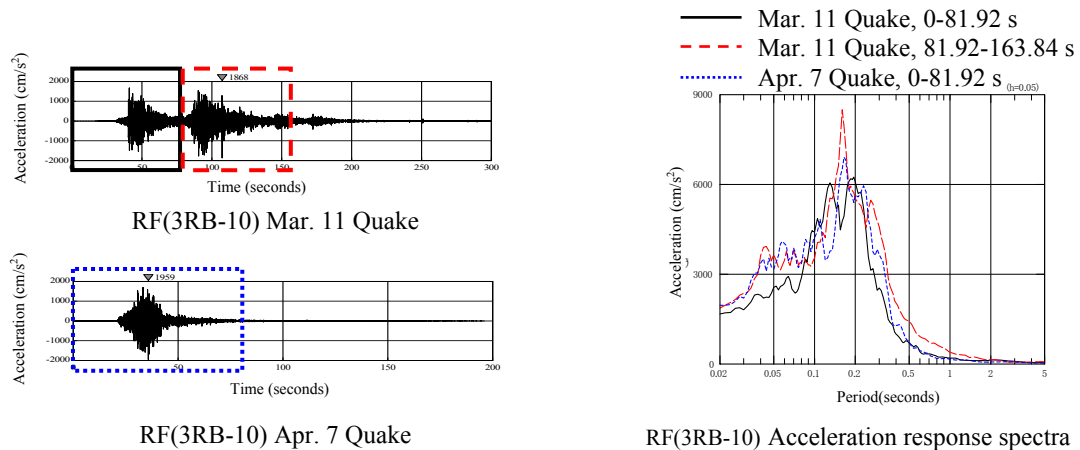


Figure 6. Comparison of Mar. 11 and Apr. 7 Quake response spectra (NS direction)

Table 1. Natural frequency changes in past major quakes

Name of Earthquake	NS direction		EV direction	
	Acceleration on base slab, 3RB-1(cm/s ²)	Frequency (Hz) Damping factor (%)	Acceleration on base slab, 3RB-1(cm/s ²)	Frequency (Hz) Damping factor (%)
Dec. 2, 2001, 22:02, South Iwate Inland M 6.4, epicenter distance 112 km	33	6.23	35	5.75
		4.29		5.25
May 26, 2003, 18:24, Miyagi Offshore M 7.1, epicenter distance 48 km	129	5.78	189	5.31
		3.95		4.51
Aug. 16, 2005, 11:46, Miyagi Offshore M 7.2, epicenter distance 73 km	222	5.55	188	5.20
		3.78		5.57
Mar. 11, 2011, 14:46, Miyagi Offshore M 9.0, epicenter distance 123 km	545	4.72	458	4.58
		6.03		7.00
Apr. 7, 2011, 23:32, Miyagi Offshore M 7.1, epicenter distance 43 km	373	4.57	398	4.48
		5.27		7.66

* Commercial operation of Onagawa NPP Unit No. 3 on Jan. 30, 2002

5.2. Observation Records Taken in Direction Orthogonal to 3F Pool Pit

Fig. 7 shows the acceleration response spectra in the direction orthogonal to the third floor pool pit (NS direction) during the March 11 Quake and April 7 Quake. In both earthquakes, the peak occurred around the 0.1-second period at the temporary observation point and was not observed at any other observation point.

We created a model incorporating the floor flexibility (in-plane deformation) of the pool pit part of the preexisting model (hereafter “partial floor spring model” [Fig. 8]) and conducted a seismic response analysis based on the observation records taken on the basemat slab, as we did in section 4. Fig. 9 compares the analysis results with the records taken at the third floor temporary observation point. It was identified that the consideration of the in-plane deformation of the floor showed an approach to a tendency of the observation records. Note, however, that the peak period at the observation point is closer to the long period side.

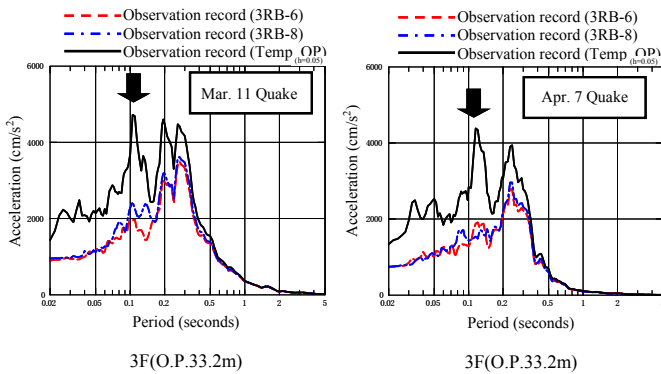


Figure 7. 3F NS-direction acceleration response spectra

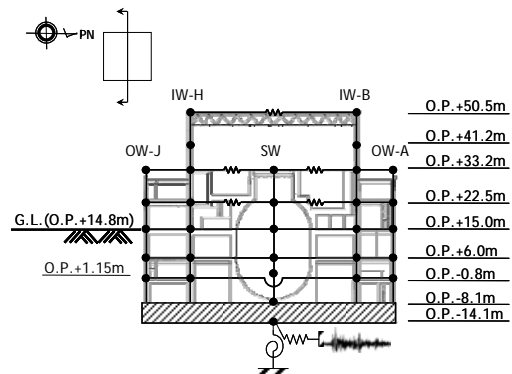


Figure 8. Partial floor spring model (NS direction)

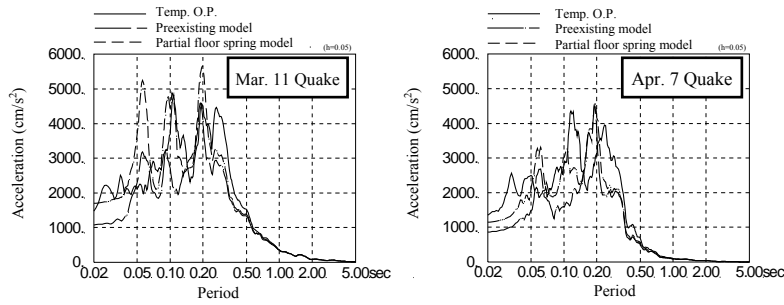


Figure 9. Acceleration response spectra (NS direction) based on partial floor spring model

5.3. Creation of Simulation Analysis Model

Based on the results of the above-mentioned consideration, the simulation analysis model of the reactor building is created as follows:

- (1) A sway-rocking model consisting of a lumped mass system and ignoring the effects of the underground surrounding soil of the side wall similarly to the preexisting model.
- (2) Because the predominant frequency is lower than those in past quakes, resulting in lower frequency responses than those in the analysis results obtained using the preexisting model, stiffness is corrected so that the natural frequency of the analysis model matches the observed/recorded predominant frequency. The stiffness is corrected by reducing the initial stiffness of the preexisting model. The stiffness equivalent to that in all time history is set even if the peak period changes between the first half and the second half as in the March 11 Quake. The non-linear characteristics associated with stiffness correction are as in Fig. 10.
- (3) The damping factor is represented by that of reinforced concrete, including that attributable to the embedment effect, to adopt values consistent with those in the observation records. Damping factor is assumed as identical in the two horizontal directions.
- (4) Floor flexibility must be taken into consideration based on the reproducibility of observation records taken in the direction orthogonal to the pool pit. Floor flexibility must be considered for the two horizontal directions on each floor.

Fig. 11 shows the simulation analysis model (before stiffness correction).

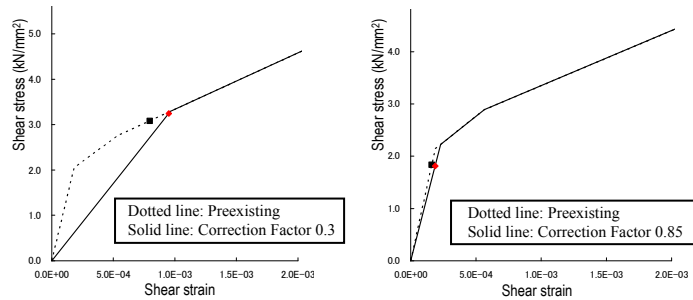


Figure 10. Method for correcting stiffness with non-linear characteristics (of typical shear skeleton)

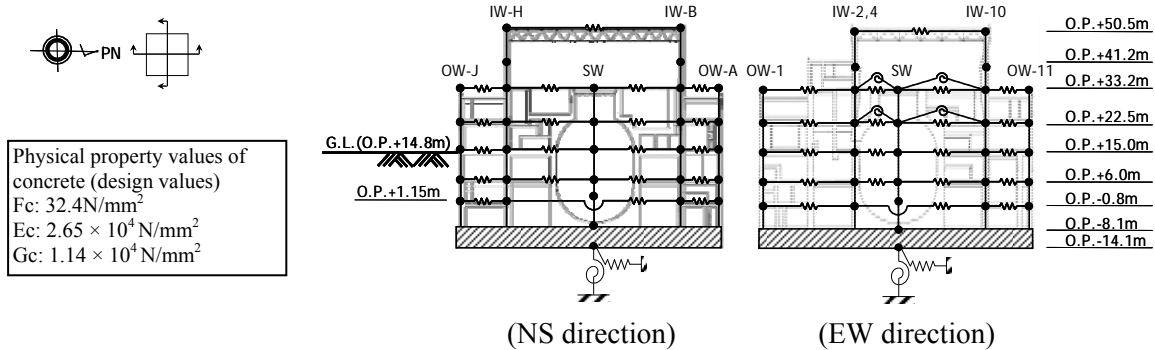


Figure 11.1. Simulation analysis model (before stiffness correction)

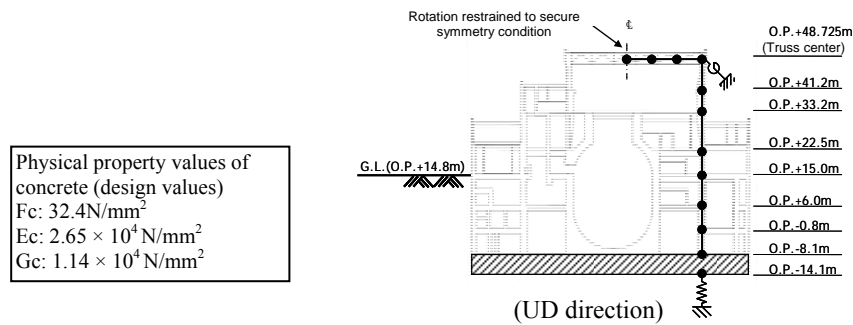


Figure 11.2. Simulation analysis model (before stiffness correction)

6. SIMULATION ANALYSIS METHOD

Using a linear analysis model, we performed a frequency response analysis based on the observation records taken on the basemat slab to inversely calculate the input motion from outside the bottom spring for nonlinear time-history seismic response analysis.

The stiffness correction factors and the RC damping factors were set based on the tendencies of transfer functions for the observation records of the March 11 Quake and April 7 Quake. The stiffness correction factors are shown in Table 2, while the transfer functions are shown in Figs. 12.

7. SIMULATION ANALYSIS RESULTS

Fig. 13 shows the maximum response acceleration distributions, Fig. 14 compares the 3F and RF acceleration response spectra with the observation records, and Fig. 15 shows the maximum response values plotted on the shear skeleton curves for the quake resisting walls. The simulation analysis results generally reproduced the observation records, and the highest maximum response shear strain was approximately 1.0×10^{-3} . The results of comparison performed just to be sure between the shear force bearable calculated from the analysis results for each quake resisting wall and the yield force bearable only by the reinforcement in the NS direction on the third floor and the Crane floor during the March 11 Quake revealed that none of the quake resisting wall reinforcement yielded (Figs. 16).

8. CONCLUSION

Using the observation records of the March 11 Quake and April 7 Quake, a simulation analysis was performed of the nuclear reactor building of Onagawa Nuclear Power Plant Unit No. 3. The use of a simulation analysis model with the floor flexibility taken into account and the building stiffness corrected allowed us to largely reproduce the observation records taken at various points in the building.

The stresses of every part of the building evaluated from the earthquake simulation analysis are confirmed to be lower than the yield value of a reinforcement. The safety of the building against the earthquakes has been confirmed with the simulation analysis.

In addition, we confirmed separately that the seismic safety is ensured to the safety related structures and equipment/piping.

REFERENCES

- Nuclear Standards Committee of JEA (Dec. 2009). Technical code for seismic design of nuclear power plants: JEAC4601-2008, The Japan Electric Association
- Tomoo Saito (Jun. 1998). System identification of a high-rise building applying multi-input-multi-output ARX model of modal analysis. *J. Struct. Constr. Eng. AIJ*, No.508,47-54.
- Yoshihiro Ogata et al. (Jun. 2011). A study of secular changes in initial stiffness of building exposed to small

and medium-scale earthquakes simulated using ARX model. *Transactions of AIJ Tohoku Chapter, JSCE, Vol. 74:* 15-18.

Table 2. Stiffness Correction Factors And Damping Factors For Simulation Analysis Model

Quake	Direction	Concrete wall stiffness correction factor (Stiffness equivalent to observations)		Damping factor (%)
		3F, Crane Floor	BF3 to BF2	
Mar. 11 Quake	NS	0.3	0.85	7
	EW	0.5	0.85	7
	UD	1.0		5
Apr. 7 Quake	NS	0.3	0.85	7
	EW	0.5	0.85	7
	UD	1.0		5

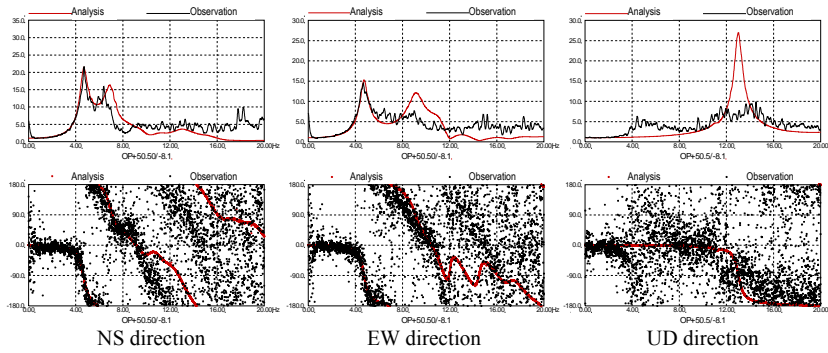


Figure 12.1. Mar. 11 Quake, transfer function, RF/Base Slab
(Upper row: amplitude, Bottom row: phase)

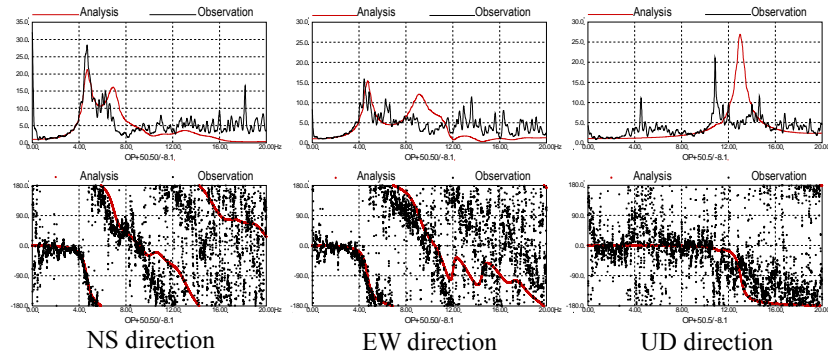


Figure 12.2. Apr. 7 Quake, transfer function, RF/Base Slab
(Upper row: amplitude, Bottom row: phase)

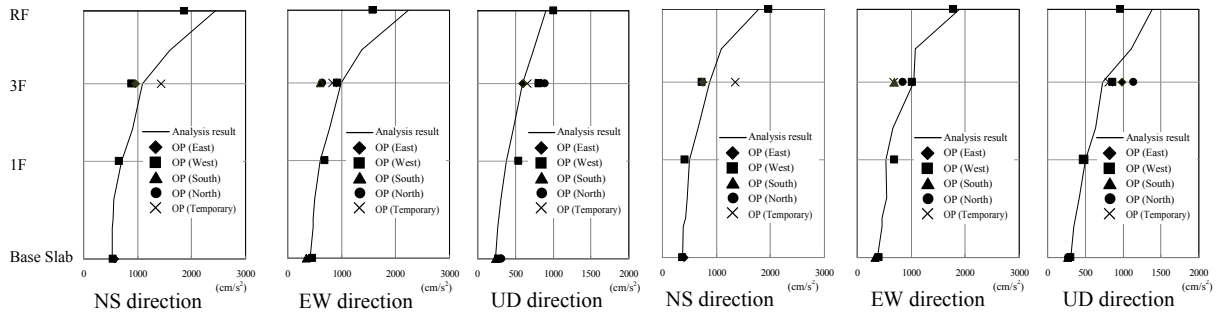


Figure 13.1. Mar. 11 Quake,
max. acceleration distribution

Figure 13.2. Apr. 7 Quake,
max. acceleration distribution

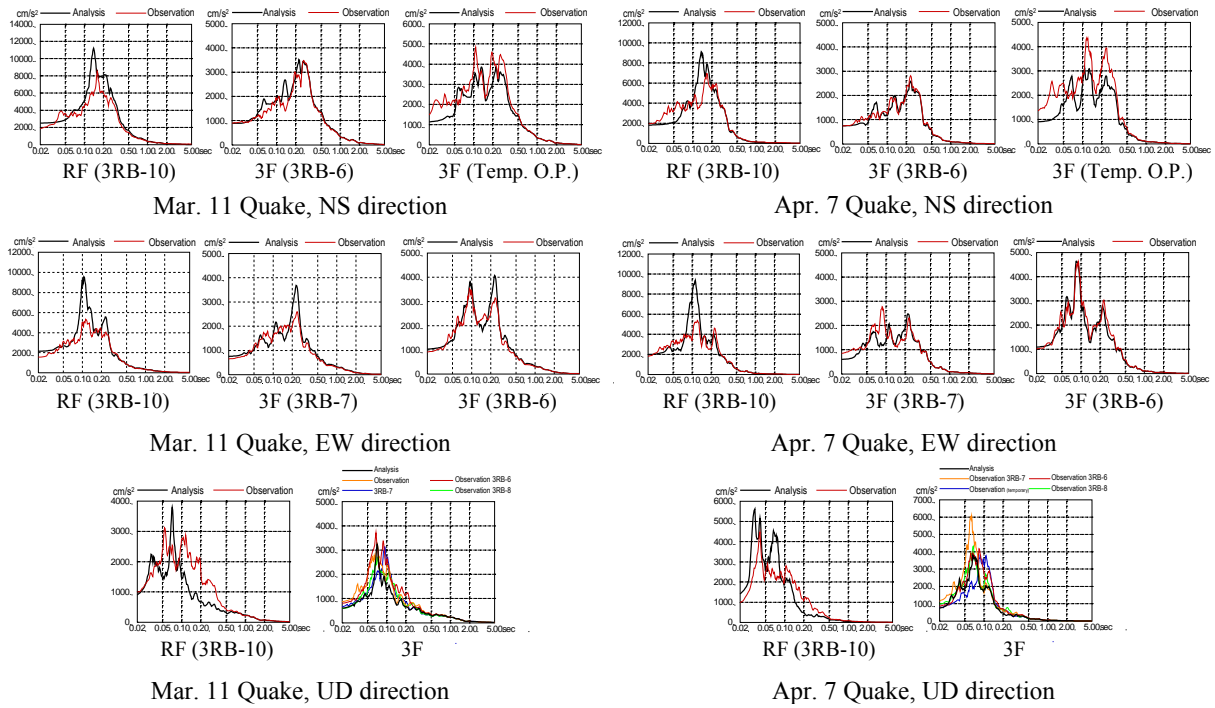


Figure 14. Comparison of acceleration response spectra

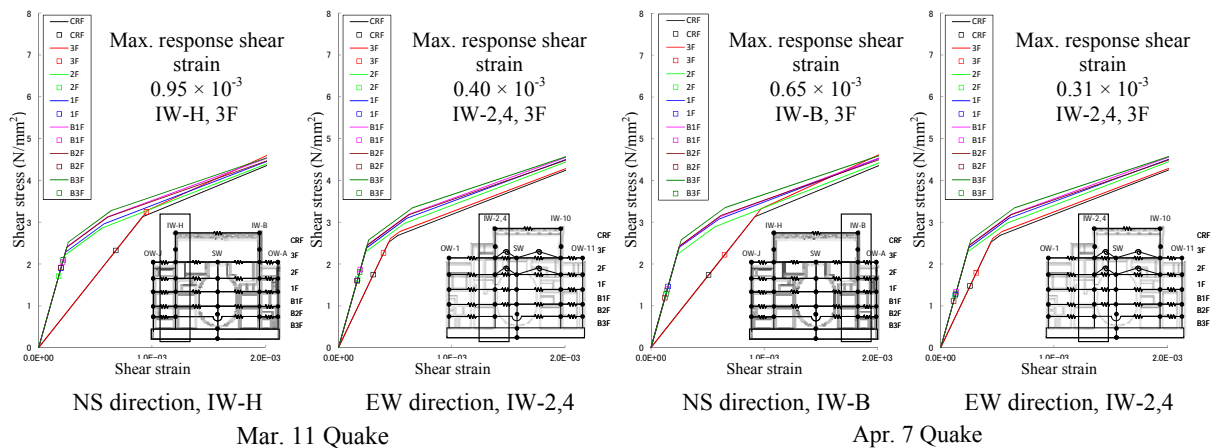


Figure 15. Max. response values plotted on shear skeleton curves

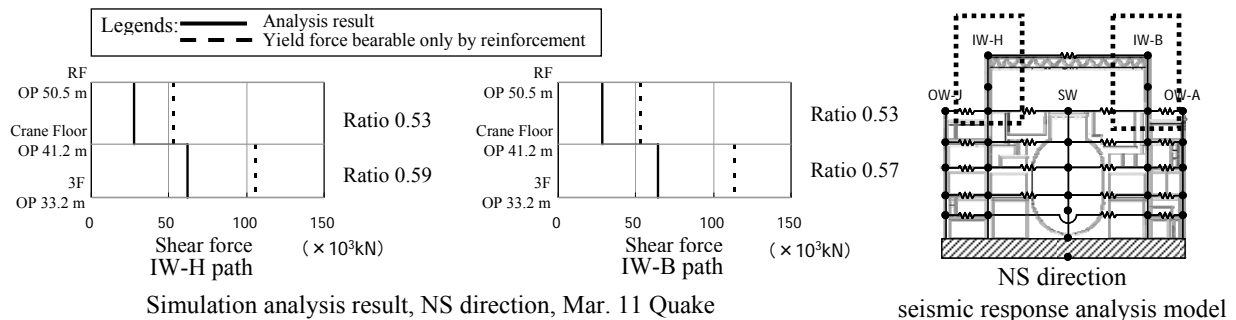


Figure 16. Shear forces on 3F and crane-floor quake resisting walls